Bacillus subtilis spreads by surfing on waves of surfactant

Thomas E. Angelini[a,1], Marcus Roper[b,1], Roberto Kolter[c], David A. Weitz[a], and Michael P. Brenner[a,1]

[a]School of Engineering and Applied Sciences, Harvard University, Cambridge, MA 02138; [b]Department of Mathematics and Lawrence Berkeley National Laboratory, University of California, Berkeley, CA 94720; and [c]Department of Microbiology and Molecular Genetics, Harvard Medical School, Boston, MA 02115

Edited by E. Peter Greenberg, University of Washington School of Medicine, Seattle, WA, and approved August 18, 2009 (received for review May 28, 2009)

The bacterium *Bacillus subtilis* produces the molecule surfactin, which is known to enhance the spreading of multicellular colonies on nutrient substrates by lowering the surface tension of the surrounding fluid, and to aid in the formation of aerial structures. Here we present experiments and a mathematical model that demonstrate how the differential accumulation rates induced by the geometry of the bacterial film give rise to surfactant waves. The spreading flux increases with increasing biofilm viscosity. Community associations are known to protect bacterial populations from environmental challenges such as predation, heat, or chemical stresses, and enable digestion of a broader range of nutritive sources. This study provides evidence of enhanced dispersal through cooperative motility, and points to nonintuitive methods for controlling the spread of biofilms.

biofilms | thin-film hydrodynamics

Bacteria bind to surfaces and to liquid–air interfaces to form biofilms, thick mats of cells cemented together by exopolysaccharides. Biofilms endow pathogenic bacteria with enhanced virulence and resistance to antibiotics. Although many recent studies have focused on the adhesins that bind bacteria to each other and to abiotic substrates (1–3) and on the signaling pathways that initiate biofilm growth (4, 5), very little is known about the physical processes by which these colonies spread over or between nutrient sources. Previous studies have highlighted the role of individual cell motility and of passive processes such as the advection of cell aggregates in propagating biofilms (6), but such propagative mechanisms depend on dispersive fluid flows. In addition to being implicated in the development of aerial structures (7), in antagonistic interactions between colonies of different bacterial species (8) the biosurfactant surfactin is known to be necessary for the spreading of colonies of *Bacillus subtilis* in the absence of external fluid flows (9, 10). However, the physical consequences of the surfactant-like behavior of surfactin on the spreading of biofilms remains unknown.

Here we show that gradients in the concentration of surfactin by cells in a liquid pellicle generates surface-tension gradients that drive cooperative spreading. The essential mechanism of surface-tension gradient-driven spreading is similar to the forced spreading of a thin film due to surface-tension gradients induced by temperature gradients (11, 12) or by exogenous surfactants (13, 14).

In the present context, a surface-tension gradient develops because of the geometry of the bacterial biofilm: The bacterial pellicle is thinner at the edge than at the center. The surfactin produced by every cell moves rapidly to the air–fluid film interface, locally reducing the surface tension. Assuming the surfactin production rate is identical for each cell, the concentration of surfactant is greater at the center of the pellicle than at the edge, which results in a gradient in surface tension that drags the film outward, away from the center of the pellicle. The gradient is self-sustained during spreading by a balance between the rate at which the clean interface is created at the advancing front of the film and the rate of surfactant supply from the center of the pellicle.

To demonstrate the mechanism of collective spreading, we first describe experiments quantifying the cooperative spreading in *B. subtilis* pellicles, including both the rate of spreading and a direct measurement of the decrease in surface tension below the center of the pellicle. We then present a mathematical model that quantitatively explains the observed spreading–both the shape of the spreading front and its velocity. The model predicts how quantities under the control of individual cells (surfactin-production rate, and biofilm rheology) control the collective motion of the biofilm. Finally, we rule out individual cell motility as the cause of the spreading by demonstrating that whereas the *B. subtilis* flagella mutant hag$^-$ does exhibit collective spreading, the surfactin mutant srfAA$^-$ does not.

Results

To expose the underlying physics of cooperative spreading, we consider a primitive spreading scenario, in which bacteria move up an inclined nonnutritive boundary. The development of a thin climbing film at the periphery of a young *B. subtilis* pellicle grown in a conical vessel partially filled with liquid medium is shown in Fig. 1. Bacteria introduced into the liquid culture in a planktonic state initially multiply and swim freely. After the oxygen in the medium is depleted, the bacteria swim or diffuse to the free surface, forming a biofilm of tightly packed cells. Approximately 12 hours after the first appearance of a pellicle of cells, a thin film of bacteria-laden fluid is dragged up the walls of the conical vessel. The speed of wall climbing is sensitive to environmental conditions but typically exceeds mm/hr, comparable with the rapid spreading of colonies due to swarming motility (15). The time dependence of the height of the biofilm as it climbs the wall is shown in Fig. 2*A*.

To demonstrate that coordinated surfactin expression drives spreading, we directly monitor the levels of surfactant by placing a 0.87-mm capillary tube near the base of the climbing film (Fig. 2*B*). The bottom end of the capillary is sealed with a dialysis membrane, which allows the nutrient medium and surfactin molecules to enter the capillary but prevents bacteria from entering. The rise height of fluid within the tube (h_r) can be related to the surface tension (γ) by balancing capillary and hydrostatic pressures below the interface:

$$\gamma \cos\theta = \frac{\rho g d h_r}{4}, \qquad [1]$$

where ρg is the weight/m^3 of the liquid medium and θ is the contact angle for liquid in the tube (16). Adsorption of surfactant to the liquid–air interface decreases γ and causes the fluid column to fall, leaving a thin film on the inside of the tube so that $\theta \approx 0$. We measure the starting height $h_r = 2.445$ cm, implying $\gamma = \gamma_0 \equiv 53$ mN/m. During the subsequent initial spreading, the height drops at the rate $\dot{h}_r = 0.87\ \mu$m/hr, implying

Author contributions: T.E.A., M.R., R.K., D.A.W., and M.P.B. designed research, performed research, contributed new reagents/analytic tools, analyzed data, and wrote the paper.

The authors declare no conflict of interest.

This article is a PNAS Direct Submission.

[1]To whom correspondence may be addressed. E-mail: angelini@seas.harvard.edu, mroper@berkeley.edu, or brenner@seas.harvard.edu.

This article contains supporting information online at www.pnas.org/cgi/content/full/0905890106/DCSupplemental.

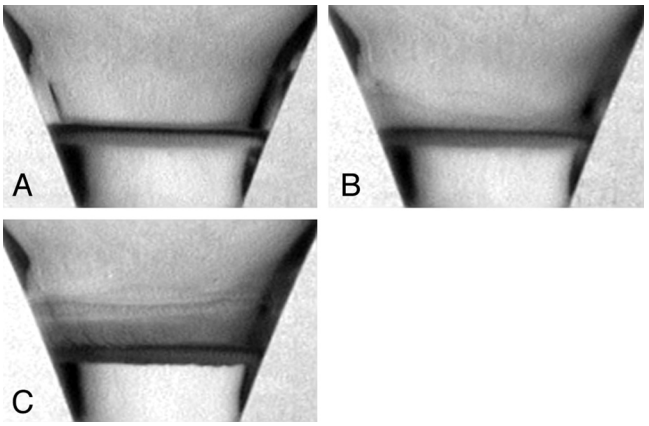

Fig. 1. Wall climbing at the edges of *B. subtilis* pellicles. Sequence of images: (*A*) Development of biofilm pellicle at an air–liquid interface. (*B*) The biofilm after the onset of wall-climbing. (*C*) The advancing film reaches a plateau length of approximately 8 mm in this example.

$\dot{\gamma} = -0.18$ mN/m·hr. Because much of the surfactant expressed by the bacteria is adsorbed onto bacterial surfaces, or into the extracellular matrix (17), actual rates of expression of surfactin may greatly exceed the rate of adsorption to the interface. The time dependence of the surface tension is compared with the height of the meniscus in Fig. 2*C*. The surface tension drops linearly in time over the first 20 hours of the experiment. After a 12-hour delay, wall climbing of the bacterial film commences, at a speed 1.39 ± 0.05 mm/hr.

Mathematical Model. The experiments demonstrate that the bacterial spreading occurs simultaneously with a drop in the surface tension. We now proceed to understand how the speed U and the thickness of the film h_∞ of the climbing bacterial film are set by the individual bacteria. Individual bacteria can control the rate of surfactin production as well as effective parameters, such as the viscosity η of the film, by modulating cell density or excreting the extracellular matrix.

We model the mixture of water and bacteria in the climbing film as a viscous Newtonian fluid with density ρ, viscosity η, and surface tension γ_0. This is an accurate description as long as exopolysaccharide (EPS) concentrations are low enough or spreading time scales are long enough that elastic stresses within the biofilm do not hinder its expansion (18). We assume that bacteria are uniformly dispersed through the film, so that the rate of surfactin accumulation at the film surface, $\dot{C}$, is controlled entirely by the local thickness. Surfactin production modifies the surface tension according to the equation of state $\gamma = \gamma_0(1 - c)$, where $c(x,t)$ is the local interfacial surfactin concentration, measured in activity units; this equation of state is valid because the surfactin concentrations in experiments during the stages of wall climbing considered here remain well below the critical micelle concentration.

Because the thickness of the climbing film, $h(x,t)$, is much smaller than the characteristic scale ℓ over which it varies, the dynamical Navier–Stokes equations reduce to the Reynolds' evolution equations for the film thickness $h(x,t)$ and $c(x,t)$ (19, 20):

$$\frac{\partial h}{\partial t} + \frac{\partial}{\partial x}\left(\frac{\gamma_0 h^3}{3\eta}\frac{\partial \kappa}{\partial x} - \frac{\rho g \cos\alpha h^3}{3\eta} + \frac{h^2}{2\eta}\frac{\partial \gamma}{\partial x}\right) = 0$$
$$\frac{\partial c}{\partial t} + \frac{\partial}{\partial x}\left(\frac{\gamma_0 c h^2}{2\eta}\frac{\partial \kappa}{\partial x} - \frac{\rho g \cos\alpha c h^2}{2\eta} + \frac{ch}{\eta}\frac{\partial \gamma}{\partial x}\right) = \dot{C}. \quad [2]$$

Here the interfacial curvature $\kappa = h_{xx}/(1 + h_x^2)^{3/2}$, where $h_x \equiv \frac{\partial h}{\partial x}$ and $h_{xx} \equiv \frac{\partial^2 h}{\partial x^2}$, g is the gravitational acceleration, and α is the inclination angle of the wall. Because any surfactant produced in the film is rapidly adsorbed to the interface, we assume that the rate of interfacial surfactant accumulation $\dot{C}$ depends only on the thickness.

Our direct measurements show that the accumulation rate asymptotes to a constant value within the colony. This cutoff is suggestive of regulation of surfactant production, either by a quorum-sensing mechanism that down-regulates surfactant expression within very dense colonies (21) or in colonies that exceed a critical thickness (22), or by localization of surfactant expression to cells that are close to the interface (23). In order to emulate this behavior, we set $\dot{C} = \dot{C}_0$ for sufficiently thick regions $h > h_{\max}$. There is no production of surfactant within regions of film that are too thin to contain bacteria. We therefore introduce a cut-off $\dot{C} = 0$ if $h < h_{\min}$. We smoothly interpolate between the two limits by using a half cosine. The observed spreading behavior is quite insensitive to the values of these bounds; in what follows, we take $h_{\max} = 0.32$ mm and $h_{\min} = 2\ \mu$m.

To quantitatively compare with experiments, we must determine the viscosity of the climbing biofilm. Although many viscometric measurements have been made for biofilms grown on solid substrates (6, 24, 25), the mechanical properties of biofilms formed at air–liquid interfaces are comparatively less well characterized. We expect the two types of biofilm to have very different viscosities. The viscosity of biofilms on solid surfaces is dominated by the excretion of the extracellular matrix, but we imaged expression of EPS by using fluorescent reporter strains from ref. 23 and found that there is, initially, no EPS expression in the climbing biofilm (see Fig. S1). This finding means that the viscosity in the climbing film is determined entirely by steric interactions between the tightly packed bacteria and by the cell density (16). We imaged the climbing biofilm and found the cells arranged in a monolayer, with a volumetric cell density of $\approx$0.6 (Fig. S1). This finding implies a fluid viscosity of $\eta = 0.2$ Pa·s (26), which is consistent with a previous measurement for a biofilm grown at an air–liquid interface (27).

We solve Eq. **2** on a one-dimensional mesh by using second-order centered finite differences to approximate the surface tension and Marangoni stress terms and upwinding for the gravitational term, and integrating forward in time by using the Matlab (Mathworks) implicit solver ode15s. We include the full expression for the capillary pressure in order to match the thin climbing

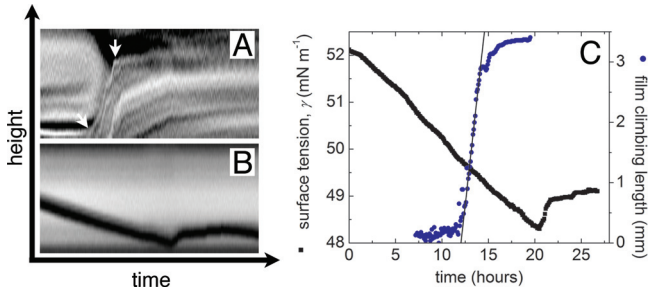

Fig. 2. Dynamics of climbing film and surfactin excretion. (*A*) Height versus time of the wall-climbing biofilm. To create this intensity map, raw transmission images were inverted to make the edge of the film look bright, and the difference of successive inverted images were taken to reduce static background and accentuating moving edges. At each time point, a region of 20 pixels was averaged horizontally, creating a map of the vertical height versus time. The arrows point to the beginning and end of the "linear" climbing region. (*B*) Height versus time of the meniscus in the capillary. The strip of pixels across the center of the capillary was averaged to create the time-lapse image. The meniscus is seen as the dark trace in the figure. The drop in meniscus height during wall climbing signals a decrease in the surface tension, consistent with surfactant production. (*C*) Plot comparing the decrease in surface tension with time (black symbols) with the increase in the wall-climbing height with time (blue symbols). Surface-tension values are extracted from the meniscus height as described in the text. The linear fit shows that the biofilm climbs at a rate 1.39 ± 0.05 mm/hr.

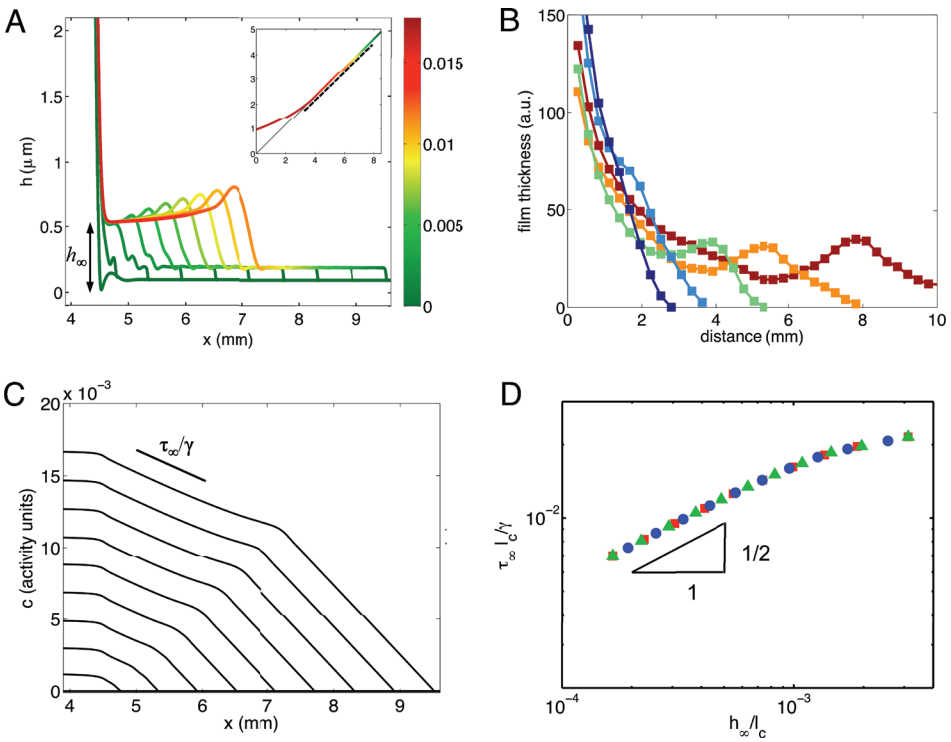

Fig. 3. A model for surfactant production in the pellicle reproduces the dynamics of the spreading bacterial film. (*A*) Simulated film thickness profiles at 40 min intervals, from 0 (left-most, blue), to 6 hours (right-most, red) after onset of wall climbing. Color coding of interface gives the surfactant concentration. $x = 0$ is the equilibrium height of the flat interface. Note the different scalings of the film thickness and rise-height axes. The *Inset* shows the entire interface and spreading front, with the magnified region indicated by the dashed reference line. (*B*) Thickness profiles (arbitrary units) from the experimental measurements of the wall climbing film at times $t = 900$ min (dark blue), 940 min (light blue), 980 min (green), 1,020 min (orange), and 1,060 min (red) after innoculation. Note the presence of the capillary ridge at the edge of the film, in striking similarity to simulations in *A*. (*C*) Simulated surfactant concentrations show a pair of Marangoni waves, one with almost constant shear τ_∞, advancing with the bacterial film, and the other advancing with the precursor film. (*D*) Film thickness and h_∞ and shear τ_∞ satisfy a compatibility condition $h_\infty/\ell_c = 3.57\ell_c^2\tau_\infty^2/\gamma_0^2$ independently of the length scale $h_{\min}$: We show collapse for $h_{\min} = 0.25\,\mu$m (red squares), $2\,\mu$m (green triangles), and $20\,\mu$m (blue circles).

film to a static meniscus, which becomes asymptotically flat at $x = 0$, and locate this static interface by solving the time-steady version of the equation ($h_t = c_t = 0$) by the shooting method (28). We regularize the dynamics of the moving contact line by assuming the wall to be wet by a very thin precursor film of thickness $b = 0.1\,\mu$m (29, 30).

The numerical solutions to these equations starting from a clean meniscus are shown in Fig. 3, for parameters corresponding to the experimentally measured surfactant production rate, inclination angle α, and initial surface tension γ_0. The model predicts that a thin film of bacteria with a thickened capillary rim advances up the wall at a constant rate (Fig. 3*A*). The inset in Fig. 3*A* shows the entire pellicle, whereas the main figure shows a blown-up version near the contact line. The climbing film is supported against surface-tension forces by an almost uniform surface-tension gradient, which is maintained by a continual supply of surfactant from the pellicle (Fig. 3*C*). The main climbing bacterial film is also preceded by a precursor film of much smaller thickness $2b$, which is supported by an almost uniform surface-tension gradient.

Scaling Analysis. The bacteria surf up the wall on self-generated surface-tension waves. The rate of spreading U and the thickness of the climbing bacterial film h_∞ depend on the two properties that individual cells have under their direct control throughout the pellicle: the rate of surfactant expression and the viscosity.

To analyze this relationship, we predict these dependencies by using a scaling analysis. Let us assume that the climbing film with thickness h_∞ and spreading velocity U is supported by a surface-tension gradient τ_∞. The surface-tension gradient in the climbing film is balanced by viscous stresses, so that

$$\tau_\infty \sim \eta \frac{U}{h_\infty}. \qquad [3]$$

Within the static meniscus, the forces that balance are surface-tension and gravitational forces: These forces require that the radius of curvature of the meniscus is given by the capillary length $\ell_c = \sqrt{\gamma_0/(\rho g \cos\alpha)}$.

To complete the analysis, we must analyze the region that matches the static meniscus to the moving film. First, following Landau and Levich (31) we require that the curvature in the climbing-film matches that of the meniscus $h_\infty/\ell^2 \sim \ell_c^{-1}$, where ℓ is the length scale on which the climbing film thickness varies. This match fixes $\ell \sim (h_\infty \ell_c)^{1/2}$. Secondly, force balance in the matching region is between viscous forces and capillarity. This balance implies that

$$\eta \frac{U}{h_\infty^2} \sim \gamma_0 \frac{1}{\ell_c \ell}. \qquad [4]$$

By combining Eqs. **3** and **4**, we can solve for h_∞ and U; we obtain (32)

$$h_\infty = a_\tau \frac{\tau_\infty^2}{\gamma_0^2}\ell_c^3, \qquad [5]$$

where the prefactor a_τ depends on the distance that the Marangoni stress extends below the equilibrium rise height of the film. In our model, this length scale is determined by $h_{\max}$, the film thickness above which the surfactant production is constant and is independent of $h_{\min}$—the thickness that the film must exceed for surfactant production to start. This scaling law is verified with our simulations in Fig. 3*D*; a fit to the scaling law implies $a_\tau = 3.57$. The different symbols collapsing in the figure are for various $h_{\min} = 0.25, 2, 20\,\mu$m. This collapse demonstrates that the wall-climbing phenotype described here is independent of the film thickness at which surfactin production commences. The gradient upon which the bacteria surf is therefore created by the static meniscus and does not either require or apparently utilize any nonlinear quorum-sensing mechanism in the film.

We calculate U and h_∞ in terms of the surfactin production rate itself. The surface tension gradient can be expressed as $\tau_\infty = -d\gamma/dx = \gamma_0 \dot{C}_0/U$. Substituting this expression into Eq. **5** then gives

$$h_\infty = a_h \left(\frac{\ell_c \eta \dot{C}_0}{\gamma_0}\right)^{1/2} \ell_c \qquad [6]$$

$$U = a_U \left(\frac{\ell_c \eta \dot{C}_0}{\gamma_0}\right)^{3/4} \frac{\gamma_0}{\eta} \qquad [7]$$

where the constants $a_h = 1.63$ and $a_U = 0.46$ can be determined from a similarity solution of the governing equations (see *Materials and Methods*). Eqs. **6** and **7** demonstrate that the thickness and speed of the climbing film depend in a nonlinear fashion on quantities that individual cells can control, the surfactin production rate and the biofilm viscosity.

Comparisons with Experiments. The simulations (Fig. 3*A*) predict that the shape of the climbing bacterial film has a characteristic bump in thickness at its edge, similar to that previously observed in thin film fluid flows driven by uniform surface tension gradients (14, 32). Strikingly, this characteristic bump is also observed in our measurements of the thickness profile of the climbing bacterial film (Fig. 3*B*), obtained by relative transmission intensities. The predicted thickness of the climbing film is $h_\infty \approx 1\ \mu$m. Although we cannot directly measure the thickness, the fact that the climbing film is a monolayer (Fig. S1) is quite consistent with this prediction.

The speed of advance and the film shape agree quite well with experimental observations. Inputting the directly measured value of $\dot{C}_0$, the predicted speed of advance is $U \approx 0.4$ mm/hr, compared with the experimental measurement of 1.4 mm/hr (Fig. 2*C*). The model's underprediction of the climbing rate likely results either from uncertainty in the true viscosity of the biofilm or from unmodeled effects of spatial variations in biofilm viscosity: We expect the bacteria to spread more rapidly if the viscosity at the edges is less than the viscosity at the center. The predicted scaling of biofilm thickness with viscosity $h_\infty \sim \eta^{1/2}$, naturally explains the observed 12-hour delay between the onset of surfactant expression and the beginning of wall climbing. For the climbing film to transport bacteria, the film thickness must exceed the thickness of a monolayer of bacteria ($\approx 0.5\ \mu$m), requiring that $\eta \gtrsim 0.1$ Pa·s. The viscosity of the bacterial pellicle increases with cell density and with the concentration of extracellular polymers expressed by the cells, and we identify the delay with the waiting time for this critical viscosity to be be reached. This mechanical thresholding intimately ties Marangoni motility to cell density, both directly, and indirectly through the quorum-sensing pathways that mediate EPS expression (22, 33).

Finally, we note that the flux of bacteria $Uh_\infty \sim \ell_c^{9/4}\dot{C}_0^{5/4}(\eta/\gamma_0)^{1/4}$, so that the flux actually increases with the viscosity of the bacteria-laden film. This behavior is in contrast to the swimming of individual cells, which typically slows as viscosity is increased (34).

The one gross contradiction between the mathematical model and the experiments is that experimentally the colony stops spreading several hours before surfactant stops being supplied to the interface. We attribute this stoppage to a change of phase at the colony edges: Simultaneous with their expression of surfactin, cells also produce a matrix of EPS which binds cells together (17). Once all cells in the colony periphery are tightly bound by this matrix, spreading is arrested. Note, however, that secondary traveling bands propagate up the wall for as long as surfactant is produced within the colony (Fig. 2*A*). Evidently, surfactant gradients continue to drive a thinner layer of fluid, which may or may not contain cells, from under the pellicle of tightly bound cells. When surfactant expression ceases, spreading of these secondary bands stops. Our measurements show that the surface tension then starts to increase, signalling either desorption of surfactant from the interface or that the entire colony has gelled (Fig. 2*C*).

Surfactin Mutants Do Not Exhibit Collective Spreading. The collective spreading of the bacterial pellicles that we have described here cannot be attributed to conventional motility, such as individual swarming or swimming (15). To confirm that the motility mechanism described here is independent of mechanisms previously described, we repeated the experiment with two mutant strains. srfAA$^-$ bacteria do not express surfactin and do not exhibit wall climbing (Fig. 4). In contrast, hag$^-$ bacteria do not have flagella, and so can not swim, but retain the surfactin-expression pathway. Strikingly, these mutants climb the wall as readily as swimming strains (Fig. 4).

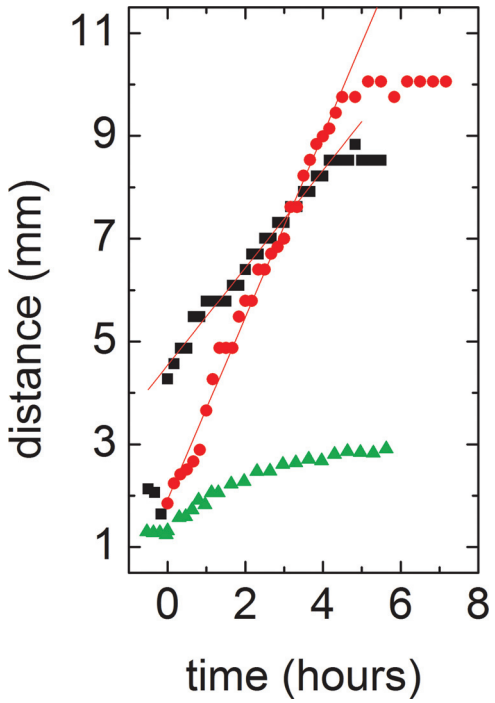

Fig. 4. Bacterial spreading rate in WT (black squares), srfAA$^-$ (surfactin knockout, green triangles) and hag$^-$ (flagellum knockout, red circles) bacteria. Both WT and mobility mutant bacteria exhibit wall climbing. Knocking out surfactin destroys the ability of the bacterial pellicle to collectively climb the wall, confirming that Marangoni stresses drive pellicle expansion, and that surfactin gradients are responsible for these stresses.

Discussion

We have presented evidence for cooperative spreading of bacterial pellicles. In contrast to previously described dispersal mechanisms, dispersal by Marangoni waves increases as the viscosity of the bacterial pellicle is increased. This discovery suggests nonintuitive strategies for controlling the spreading of biofilms. Biosurfactant coatings are already known to limit biofilm growth in some circumstances, but the effect has previously been attributed to their inferred antibiotic action (35). Inhibition of Marangoni waves provides an alternative physical explanation for the retardation of spreading. Coating the wall with surfactant increases its wettability but may nonetheless make it harder to climb by saturating the interface of the rising film or even imposing a Marangoni stress that opposes the surfactant wave generated by the bacteria. The cooperative basis of this form of dispersal also merits further scrutiny—our simulations show that the cells that surf the Marangoni wave do not themselves need to produce surfactant, so that cells in the center may find themselves paying the entire fitness cost of expressing surfactant without enjoying access to new substrates. Marangoni motility may therefore provide a new paradigm for studying the evolutionary stability of a costly form of cell-to-cell cooperation with nontargeted benefits.

Materials and Methods

Bacterial Strains and Growth. To grow the biofilm pellicles, we adapt the protocols in ref. 7. Strain 3610 *B. subtilis* cells are streaked from a −80°C freezer stock onto an LB medium plate, 1.5% agar. The plates are incubated at 37°C for twelve hours. Three milliliters of LB liquid medium is inoculated with cells from an isolated colony on the plate. The inoculated LB medium is incubated on a shaker at 37°C for three hours, when the optical density of the bacteria solution is approximately 0.6. Forty microliters of the bacteria solution is added to 4 mL of minimal salts glycerol glutamate medium (7) in a

sterile conical vessel. The vessel is covered and placed in a humidified chamber, maintained at a temperature of 30°C. Images are collected for several days at a frame rate of once per five minutes and postprocessed with custom software. The knockout strains are also *B. subtilis* 3610 with srfAA::mls and hag::tet mutations.

Similarity Analysis. To find the dimensionless coefficients in Eqs. **6** and **7**, we write Reynolds' equations in similarity form $h(x,t) = h_\infty H(\xi, T)$, $c(x,t) = (\dot{c}_\infty \ell/U)TC(\xi, T)$, where $\xi = X/T$ is our similarity variable, and $T = Ut/\ell$, and $X = (x - \sqrt{2}\ell_c)/\ell$ are the dimensionless counterparts to t and x (20). Both gravitational forces and surfactin expression within the thin film is negligible: The Marangoni wave is maintained by surfactant supplied to the film from the pellicle itself. The resulting equations are then integrated numerically subject to boundary conditions $C = 0$, $H = b$ as $\xi \to \infty$, and $C = 1$ at $\xi = 0$. A final constraint arises from the requirement of compatibility of shear stress and film thickness where the film meets the static meniscus: $H_\infty = a_\tau(\partial C/\partial\xi)^2$.

We obtain $a_\tau = 3.57$ from our simulations (Fig. 3*C*); self-generated Marangoni waves therefore produce films 25% thinner than imposed uniform surface stresses (36). We evolve the equations to late times by using similar numerical routines to Eq. **2**, and obtain for the coefficients $a_h = 1.63$ and $a_U = 0.46$ from the thickness of the climbing film at $\xi = 0$ and location of the capillary ridge respectively.

ACKNOWLEDGMENTS. We thank Hera Vlamakis (Harvard University) for help and for strains, Steve Branda and Panadda Dechadilok for early experimental investigations, and Rachel Levy and Andrea Bertozzi for useful discussions. We gratefully acknowledge the BASF research initiative at Harvard University for funding this research. M.R. is supported by a fellowship from the Miller Institute for Basic Research in Sciences.

1. Heilmann C, et al. (1996) Molecular basis of intercellular adhesion in the biofilm-forming *Staphylococcus epidermidis*. *Mol Microbiol* 20:1083–1091.
2. Klapper I, Dockery J (2006) Role of cohesion in the material description of biofilms. *Phys Rev E* 74:031902.
3. Wang X, Preston J, Romeo T (2004) The *pgaABCD* locus of *Escherichia coli* promotes the synthesis of a polysaccharide adhesin required for biofilm formation. *J Bacteriol* 186:2724–2734.
4. O'Toole G, Kolter R (1998) Initiation of biofilm formation in *Pseudomonas fluorescens* wcs365 proceeds via multiple, convergent signalling pathways: A genetic analysis. *Mol Microbiol* 28:449–461.
5. Koutsoudis M, Tsaltas D, Minogue T, von Bodman S (2006) Quorum-sensing regulation governs bacterial adhesion, biofilm development, and host colonization in *Pantoea stewartii* subspecies *stewartii*. *Proc Natl Acad Sci USA* 103:5983–5988.
6. Hall-Stoodley L, Costerton JW, Stoodley P (2004) Bacterial biofilms: From the natural environment to infectious diseases. *Nat Rev Microbiol* 2:95–108.
7. Branda S, González-Pastor JE, Ben-Yahudar S, Losick R, Kolter R (2001) Fruiting body formation by bacillus subtilis. *Proc Natl Acad Sci USA* 98:11621–11626.
8. Straight P, Willey J, Kolter R (2006) Interactions between *Streptomyces coelicolor* and *Bacillus subtilis*: Role of surfactants in raising aerial structures. *J Bacteriol* 188:4918–4925.
9. Kinsinger R, Shirk MC, Fall R (2003) Rapid surface motility in *Bacillus subtilis* is dependent on extracellular surfactin and potassium ion. *J Bacteriol* 185: 5627–5631.
10. Kinsinger RF, Kearns DB, Hale M, Fall R (2005) Genetic requirements for potassium ion-dependent colony spreading in bacillus subtilis. *J Bacteriol* 187:8462–8469.
11. Cazabat A, Heslot F, Troian S, Carles P (1990) Fingering instability of thin spreading films driven by temperature gradients. *Nature* 346:824–826.
12. Brzoska J, Brochard–Wyart F, Rondelez F (1992) Exponential growth of fingering instabilities of spreading films under horizontal thermal gradients. *Europhys Lett* 19:97–102.
13. Jensen O, Grotberg J (1992) Insoluble surfactant spreading on a thin viscous film: Shock evolution and film rupture. *J Fluid Mech* 240:259–288.
14. Bertozzi A, Münch A, Fanton X, Cazabat A (1998) Contact line stability and "undercompressive shocks" in driven thin film flow. *Phys Rev Lett* 81:5169–5172.
15. Kearns D, Losick R (2003) Swarming motility in undomesticated *Bacillus subtilis*. *Mol Microbiol* 49:581–590.
16. Batchelor G (1967) *Introduction to Fluid Dynamics* (Cambridge Univ Press, Cambridge, UK).
17. Sutherland I (2001) The biofilm matrix–an immobilized but dynamic microbial environment. *Trends Microbiol* 9:222–227.
18. Klapper I, Rupp C, Cargo R, Purvedorj B, Stoodley P (2002) Viscoelastic fluid description of bacterial biofilm material properties. *Biotechnol Bioeng* 80:289–296.
19. Edmonstone B, Matar O, Craster R (2004) Flow of surfactant-laden thin films down an inclined plane. *J Eng Math* 50:141–156.
20. Levy R, Shearer M (2006) The motion of a thin liquid film driven by surfactant and gravity. *SIAM J Appl Math* 66:1588.
21. Sullivan ER (1998) Molecular genetics of biosurfactant production. *Curr Opin Biotech* 9:263–269.
22. Chopp D, Kirisits M, Moran B, Parsek M (2003) The dependence of quorum sensing on depth of a growing biofilm. *Bull Math Biol* 65:1053–1079.
23. Vlamakis H, Aguilar C, Losick R, Kolter R (2008) Control of cell fate by the formation of an architecturally complex bacterial community. *Gene Dev* 22:945–953.
24. Lau P, Dutcher J, Beveridge T, Lam J (2009) Absolute quantitation of bacterial biofilm adhesion and viscoelasticity by microbead force spectroscopy. *Biophys J* 96:2935–2948.
25. di Stefano, et al. (2009) Viscoelastic properties of *Staphylococcus aureus* and *Staphylococcus epidermidis* mono-microbial biofilms. *Microb Biotechnol*, 10.1111/j.1751-7915.2009.00120.x.
26. Verberg R, de Schepper I, Cohen E (1997) Viscosity of colloidal suspensions. *Phys Rev E* 55:3143–3158.
27. Koza A, Hallett P, Moon C, Spiers A (2009) Characterization of a novel air-liquid biofilm of *Pseudomonas fluorescens*. *Microbiology* 155:1397–1406.
28. Press W, Teukolsky S, Vetterling W, Flannery B (2007) *Numerical Recipes: The Art of Scientific Computing* (Cambridge Univ Press, Cambridge, UK), 3rd Ed.
29. Troian S, Herbolzheimer E, Safran S (1990) Model for the fingering instability of spreading surfactant drops. *Phys Rev Lett* 65:333–336.
30. Brenner M, Bertozzi A (1997) Linear instability and growth of driven contact lines. *Phys Fluids* 9:530–539.
31. Landau L, Levich B (1942) Dragging of a liquid by a moving plate. *Acta Physicochim USSR* 17:42–54.
32. Fanton X, Cazabat A, Quéré D (1996) Thickness and shape of films driven by a marangoni flow. *Langmuir* 12:5875–5880.
33. Davies D, et al. (1998) The involvement of cell-to-cell signals in the development of a bacterial biofilm. *Science* 280:295–298.
34. Schneider W, Doetsch R (1974) Effect of viscosity on bacterial motility. *J Bacteriol* 117:696–701.
35. Rodrigues L, van der Mei H, Teixeira J, Oliveira R (2004) Biosurfactant from *Lactococcus lactis* 53 inhibits microbial adhesion on silicone rubber. *Appl Microbiol Biotechnol* 66:306–311.
36. Schwartz L (2001) On the asymptotic analysis of surface-stress-driven thin-layer flow. *J Eng Math* 39:171–188.